LAWRENCE
LIVERMORE
NATIONAL
LABORATORY

LLNL-JRNL-413180

Geometrical frustration in an element solid: (beta)-rhombohedral boron

T. Ogitsu, F. Gygi, J. Reed, M. Udagawa, Y. Motome, E. Schwegler, G. Galli

May 20, 2009

Physical Review B

Disclaimer

Geometrical frustration in an elemental solid: β-rhombohedral boron

Tadashi Ogitsu*[1], François Gygi[1,2], John Reed[1], Masafumi Udagawa[3], Yukitoshi Motome[3], Eric Schwegler[1], and Giulia Galli[1,2]

[1]*Lawrence Livermore National Laboratory, CA, USA;*
[2]*University of California, Davis, CA, USA;*
[3]*University of Tokyo, Tokyo, Japan.*
**ogitsu@llnl.gov*

Although a comprehensive understanding of the basic properties of most elemental solids has been achieved, there are still fundamental, open questions regarding simple substances, e.g. boron. Based on an Ising model that describes the intrinsic defect states in elemental boron, we show that this system is the only known element to exhibit geometrical frustration in its solid form. Interestingly, we find that the peculiar transport properties of boron that have been reported over the past forty years originate from the presence of geometrical frustration.

Elemental boron was first isolated in its pure form nearly a hundred years ago, a century after the discovery of the fifth element[1]. However, as recently pointed out in several studies[2,3,4], the phase diagram of boron and its most stable allotrope under ambient conditions are still poorly understood[5]. Intrinsic defects have been shown to be responsible for making β-rhombohedral boron the most stable phase[3,4] down to temperature very close to zero; however, no long-range ordering of these defects has ever been found experimentally, and theory suggests that there are a macroscopic number of nearly degenerate ground state configurations[4]. These findings are seemingly at odds with what one would expect based on the third law of thermodynamics. We propose that many of the peculiar properties of solid boron arise from the fact that this element has a nearly degenerate ground state *due to geometrical frustration*.

The most well known example of geometrical frustration is the proton disordered ice Ih, whose structure was first rationalized by L. Pauling in 1935[6]. In the 1990s, spin systems represented by magnetic pyrochlore materials were shown to have geometrical frustration similar to that of ice[7,8]. In particular, the proton disorder in ice and spin magnetism in magnetic pyrhochlore materials share the same underlying model[7], the ferromagnetic Ising model on a corner sharing tetrahedron. This model, within the nearest neighbor (NN) interaction approximation, has an exactly degenerate and disordered ground state with a macroscopic zero point entropy that agrees surprisingly well with estimates based on experimental specific heat measurements. However, recent studies support the notion that the measured macroscopic residual entropy corresponds to a non-equilibrium state due to slow dynamics at low temperature, and thus, the third law of thermodynamics is unlikely to be violated[8]. Nevertheless, it was the identification of underlying model Hamiltonians that paved the road to the understanding of the complex behavior of frustrated systems[6,7,9].

In this paper, we report on the first known case of geometrical frustration in an elemental solid. In particular, we show that the imperfect atomic occupation in the elemental boron crystal, known as partial occupancy, can be modeled by an anti-ferromagnetic (AF) spin Ising model on an expanded kagome lattice[10,11], whose ground state is exactly degenerate and disordered. Therefore, boron bears striking similarities to ice and spin ice, with a nearly degenerate ground state. We also show that the rather peculiar transport properties of boron that have been reported over the past forty years[12,13,14,15] can be rationalized by presence of geometrical frustration.

Upon slow cooling, liquid boron solidifies into the β-rhombohedral phase,[16] which has an unusually large unit cell, approximately 320 atoms per hexagonal cell (hex-cell hereafter). In this structure, six out of twenty crystallographic sites are only partially occupied (partially occupied site, POS) with occupation rates varying from 2% to 75% from site to site (23 out of 320 atoms are at POS)[16]. The topology of POS, determined by experiments, corresponds to a "quasi" 2D expanded kagome lattice[10] of the double layer type (Fig. 1).

We have previously shown that the occupancy of POS, *i.e.* the distribution of unoccupied and occupied sites, can be mapped onto a generalized spin Ising model:[4]

$$H = \sum_i U_i S_i + \sum_{i,j} J_{i,j} S_i S_j + \sum_{i,j,k \in B13} T_{i,j,k} S_i S_j S_k + C \quad , \quad (1)$$

where, S_i is the occupation at site i, which takes values of either +1 (occupied) or -1 (occupied), U_i is the site dependent local potential, $J_{i,j}$ is the pair interaction between sites, i and j, $T_{i,j,k}$ are three body interactions, and the sum is limited within the same B_{28} unit (see Figure 1a). C is a constant parameter.

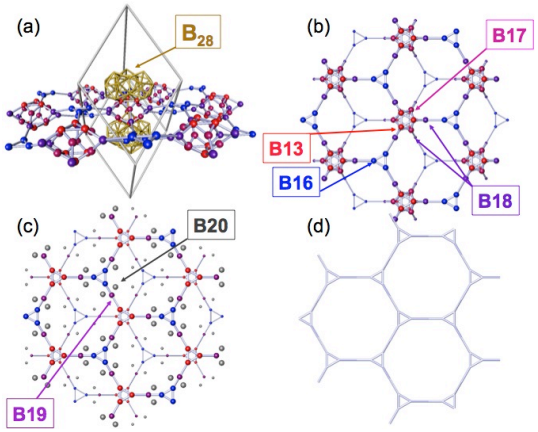

Figure 1: The lattice structure of Partially Occupied Sites (POS) in β-rhombohedral boron. (a) The POS forms a layered lattice structure at z=0 (not drawn), and z=c/2 (drawn), where c is the lattice parameter of a rhombohedral crystal. Two clusters made of 28 boron atoms (B_{28}, gold bonds) are connected by an interstitial atom and B13 vacancies (red spheres), and they are located in the middle of the rhombohedral cell. (b) and (c) depict the connectivity between B13, B16-B20. B13 (red), B16 (blue), B17 (magenta) and B18 (purple) are displayed in (b), and the rest, B19 (purple) and B20 (grey) are displayed in (c) separately for the sake of clarity. The viewpoint is from z-axis, and the size of spheres and bonds correspond to the offset in the z-axis. (d) A single layer of this lattice, an expanded kagome lattice, is depicted, where the corners of the hexagonal lattice are decorated by triangles. The POS lattice of β-boron consists of two layers of expanded kagome lattices connected to each other through the B13 site. For a more detailed explanation, see refs. [4,16].

The interaction coefficients *U, J, T,* and *C* were fitted to *ab-initio* total energy calculations of β-boron, carried out for an extensive amount of independent POS occupation configurations, and using different sizes of unit-cells (rhombohedral cell and 1280 atom supercell). The resulting model reproduces the *ab-initio* total energies to within a few meV/atom (see ref. [4] for details) and favors the β phase over the α phase, in agreement with previous studies[3]. Remarkably these calculations demonstrated that the presence of intrinsic defects significantly lowers the internal energy of β-boron due to the peculiar chemical properties of this element, which tends to form three-centre, two-electron bonds[4]. Interestingly, all of the nearest neighbor (NN) interactions in Eq. (1) (the β-boron Ising model hereafter) are anti-ferromagnetic (AF) except for the pairing occupation at B17 and B18 sites (see Fig. 1 for site definitions). Given the crucial role that the simplest NN Ising models played in the development of the theory of frustration[6,7,9], we first examined a simplified version of the β-boron Ising model, that is a NN AF Ising model on an expanded kagome lattice[10]. The ground state of this model is essentially equivalent to that of the NN AF Ising model on the kagome lattice, which is exactly degenerate and disordered [17]. A simple mapping that shows the equivalence of the ground state properties of those two models is illustrated in Fig. 2.

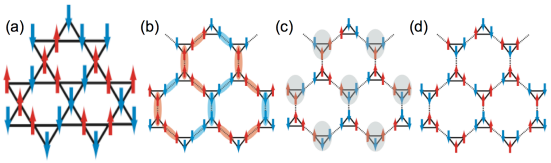

Figure 2: Schematic illustrations describing the equivalence between the ground states of the AF Ising model on an expanded kagome lattice and that on the kagome lattice. In (a), one of the ground state spin configurations of AF Ising model on a kagome lattice is realized, which is described as "two-up one-down" or "two-down one-up" spin configurations, maximizing the number of opposite spins on a triangle. The expanded kagome lattice is made by decorating the corner of hexagonal rings with triangles. If one duplicates the spins on the kagome lattice, (a), onto the spins on an expanded kagome lattice, (b) is obtained. Choose half of the triangles in an alternating manner (shaded triangles in (c)), and flip the spins on the shaded triangles, (d). The resulting spin configuration in (d) gives the ground state of the AF Ising model on the expanded kagome lattice, since all the inter-triangle bonds are AF in addition to "two-up one-down" rule for the spin configuration on each triangle.

We now turn to the thermodynamic properties of the β-boron Ising model (Eq. 1). The model Hamiltonian, which was originally developed to reproduce the first-principles DFT total energies of β-rhombohedral boron quantitatively[4], required a large number of interaction parameters (40 in total). Therefore, it is extremely challenging to examine it directly with an analytical approach. Here, we employed a numerical approach based on the replica exchange Monte Carlo (REMC) method, which was developed to overcome slow dynamics at low temperatures[18]. In this method, many MC runs on a discretized temperature grid are performed, and exchanging configurations at adjacent temperatures are repeatedly attempted with an algorithm that ensures

detailed balance[18]. As a consequence, all configurations repeatedly undergo high temperature annealing cycles. In the present case, the occupation state at each site turned out to change on average by 18% after one REMC cycle at the lowest temperature, demonstrating the effectiveness of the approach.

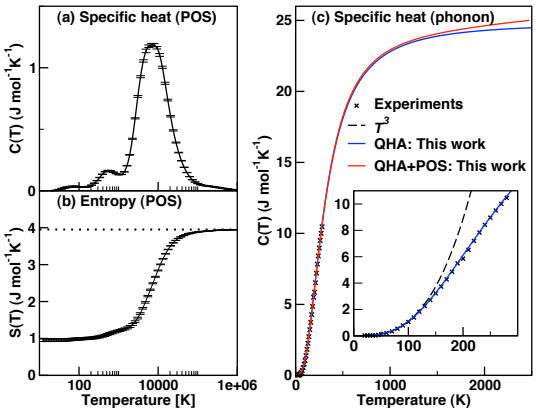

Figure 3: (a) Specific heat of the Ising model fit to *ab-initio* data, including error bars, as a function of temperature. (b) Entropy as a function of temperature calculated by thermodynamic integration from the high temperature limit. The data were obtained for a 4x4x6 supercell (4,032 sites) derived from the rhombohedral-cell. The solid lines in (a) and (b) are guides to the eye. The horizontal dotted line in b) is the high temperature limit of the entropy, $S(T\to\infty) = -R(p_{occ}\log p_{occ} + p_{unocc}\log p_{unocc})$, where, p_{occ} is the occupation rate (23/126), p_{unocc}=1-p_{occ}, and R is the gas constant. We obtained 1280 data points, and only ten percent (with error bars) are plotted for clarity. (c) Measured specific heat (crosses)[19], together with calculated phonon specific heat (blue line) and the sum of phonon and configurational specific heats (red line). The temperature range below 300K is magnified in the inset.

The specific heat of the β-boron Ising model was calculated on a temperature grid between 11.6K and 1.16×10^9 K (see Fig. 3a) at a fixed occupation rate p_{occ}=*23/126,* which corresponds to the experimental atomic density[16]; an analytical high temperature expansion form ($\propto T^{-2}$) was used for extrapolation to infinite temperature. Thermodynamic integration was performed to calculate the entropy as a function of temperature, using infinite temperature as the reference point (see Fig 3b). Within the system sizes considered here, corresponding to 2x2x3, 3x3x3 and 4x4x6 repetitions of the rhombohedral cell, we did not observe any evidence of phase transitions, and the calculated specific heat for each cell size was in agreement within statistical error bars. As can be seen in Fig 3b, the β-boron Ising model has a macroscopic amount of entropy, roughly ¼ of the high temperature limit, at the lowest temperature of our simulation. In our simulations, when the temperature decreases from the high T limit, first a large variation in the POS occupation rate is observed at 2000-10000K; most of the short-range correlations observed in our calculations develop in this temperature range. Subsequently, the interstitial B19/B20 occupation (see Fig.1 for definition of specific sites) gradually decreases, while the number of B17-B18 pairs (see Fig.1) remains roughly constant. Below 200 K, the relative locations of B16 interstitials are gradually optimized against the orientation of B13 vacancies and its occupied pairs such as a B17-B18 pair, a B19, or a B20. This sequence of geometrical arrangements corresponds to three peaks in the specific heat.

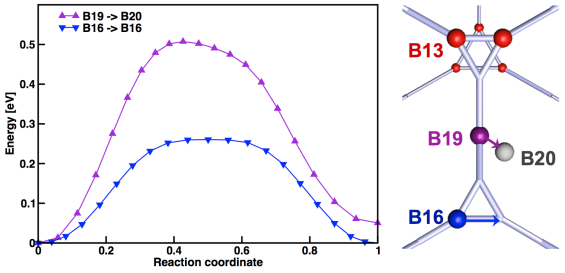

Figure 4: The total energy eV per rhombohedral-cell along the reaction coordinates of the two lowest energy barrier paths. The B16 → B16 diffusion (the blue arrow) corresponds to the intra-triangle diffusion along a symmetric direction with respect to the B19 atom. The B19→B20 diffusion (the purple arrow) takes place with the far side B16 site occupied (as drawn).

The configurational constant volume specific heat, *C(T)*, of spin ice has been measured precisely, and this contributed significantly to the development of the theory of frustration in spin ice[8]. Unfortunately the *C(T)* of β-boron has not been as extensively studied, and the separation of configurational and vibrational contributions has never been attempted. The vibrational specific heat calculated from our first-principles phonon density of states is shown in Fig. 3c and is in excellent agreement with experiments[19], including the T^3 behavior below *T=100 K* and the non-T^3 behavior above this temperature. A small scatter in the experimental data for *C(T)* at *T~200K* can be seen, although it is not clear if the scatter is within experimental uncertainties or if it corresponds to a dynamical temperature induced change in POS configuration.

Apart from the specific heat, we found that there are several experimental evidences that the POS atoms diffuse over a wide range of temperature, whose potential relation to geometrical frustration has never been discussed. For example, Tsagareishlili *et al.* performed internal friction experiments over a range of temperatures (*77K* to *1000K*)[13], and found two clear

peaks of inelastic response at *T=150K* and at *T=530K*,[13] indicating the presence of defect diffusion processes in β-boron. Werheit and Wehmoller measured the relaxation behavior in conductivity data, and identified the presence of various relaxation mechanisms down to *T~100K*, which was attributed to boron diffusion processes[15].

In order to examine a connection between the observed boron diffusion and the near degenerate POS configuration due to geometrical frustration, we have calculated the energy barriers between several different POS occupation configurations among of the lowest energy structures found in ref [4] from first-principles, using the elastic band method[20]. We have identified two low-activation diffusion paths connecting (near) degenerate low energy POS occupation configurations (see Fig. 4): inter B16 hopping and B19-B20 hopping, with barriers of 0.25eV and of 0.5eV, respectively (see Figs. 1 and 4 for site definitions), in qualitative agreement with the experiments[13]. All the other diffusion paths, particularly, the ones that change the location of B13 vacancies have high activation barriers (several eV) higher than the melting temperature (~2350K) of β-boron. An autocorrelation function analysis of the Ising model Monte Carlo calculations, in addition to the calculated activation barriers, leads to the following conclusion. Hopping between B19 and B20 can still take place at around *T=600K* (or the temperature range corresponding to the middle peak in *C(T)*), while below *T=200K*, only inter B16 hopping takes place. This suggests that the two diffusion processes at *T=150K* and *T=530K*, inferred from the internal friction experiments[13], correspond to these two hopping mechanisms. Based on our simulation results, we also suggest that the change in the optical absorption observed around *T=150~200K*[14] can be attributed to the inter B16 hopping, and the introduction of gap levels due to an unfavorable B16 occupation configuration[4].

In summary, we have demonstrated that the partial occupancy of β-rhombohedral boron is described by an AF Ising model on a double layer expanded kagome lattice, which possesses a (nearly) degenerate ground state due to geometrical frustration. We have also provided computational evidence to support the interpretation that the observed boron diffusion processes correspond to dynamical reconfigurations of POS atoms between near degenerate ground states.

We thank Dr. Leonardo Spanu (UC Davis, USA) for stimulating discussions and useful suggestions. This work was performed under the auspices of the U.S. Department of Energy by Lawrence Livermore National Laboratory under Contract DE-AC52-07NA27344 and partially supported by DOE/Scidac grant no. DE-FG02-06ER46262.

[1] Weeks, M. *Discovery of the elements* pp.540-555 (University Microfilms International, A Bell & Howell Company, Ann Arbor, Michigan, USA, 1993).

2 D. L. V. K. Prasad, M. M. Balakrishnarajan and E. D. Jemmis, *Phys. Rev. B* **72**, 195102 (2005); A. Masago, K. Shirai, and H. Katayama-Yoshida, *Phys. Rev. B* **73**, 104102 (2006); S. Shang, Y. Wang, R. Arroyave, and Z.-K. Liu, *Phys, Rev. B* **75**, 092101 (2007).

3 M. J. van Setten, M. A. Uijttewaal, G. A. de Wijs and R. A. de Groot, *J. Am. Chem. Soc.* **129**, 2458 (2007); M. Widom, M. Mihalkovic, *Phys. Rev. B* **77**, 064113 (2008).

4 T. Ogitsu, T., F. Gygi, J. Reed, E. Schwegler, Y. Motome, and G. Galli, *J. Am. Chem. Soc.* **131**, 1903 (2009).

5 D. A. Young, Phase diagrams of the elements Ch. 7 (University of California Press, Berkeley and Los Angels, California; Oxford, England, 1991).

6 L. Pauling *J. Am. Chem. Soc.* **57**, 2680 (1935).

7 M. J. Harris, S. T. Bramwell, D. F. McMorrow, T. Zeiske, and K. W. Godfrey, *Phys. Rev. Lett.* **79**, 2554 (1997).

8 S. T. Bramwell and M. P. Gingras, *SCIENCE* **294**, 1495 (2001).

9 P. W. Anderson *Phys. Rev*. **102**, 1008 (1956).

10 M. E. Fisher *Phys. Rev.* **113**, 969 (1959).

11 Y.-Zh Zheng, *et al. Angew. Chem. Int. Ed.* **46**, 6076 (2007).

[12] W. P. Lonc, V. P. Jacobsmeyer, *Boron* **2**, 215, G. K. Gaule, Ed. (Plenum Press, New York, 1965).

13 G. T. Tsagareishivili, F. N. Tavadzf, G. Sh. Darsavelidze, and V. Sh. Metreveli, *Boron* **3**, 281, T. Niemyski, Ed. (Polish Scientific Publishers, Warsaw, 1970).

14 H. Werheit and R. Franz *Phys. Stat. Sol. (b)* **125**, 779 (1984), and references therein.

15 H. Werheit and B. Wehmoller, *J. Solid State Chem.* **177**, 556 (2004).

16 G. A. Slack, C. I. Hejna, M. F. Garbauskas and J. S. Kasper *J. Solid State Chem.* **76**, 5 (1988).

17 I. Syozi *Prog. Theor. Phys*. **6**, 306 (1951).

18 K. Hukushima and K. Nemoto *J. Phys. Soc. Jpn*. **65**, 1604 (1996).

19 V. I. Bogdanov, Yu. Kh. Vckilov, G. V. Tsagareishvili and I. M. Zhgenti *Sov. Phys.-Solid State* **12**, 2701 (1971).

20 We used PWSCF version 4 (www.pwscf.org) using the same calculation conditions used in Ref [4], except that the PBE GGA is used in this work.